IOP Conf. Series: Journal of Physics: Conf. Series **847** (2017) 012069 doi:10.1088/1742-6596/847/1/012069

Computational simulations of the influence of angular rotation deviations in optical CT imaging of gel dosimeters

Yi Du[1, 2], Gongyi Yu[1, 3], Xincheng Xiang[1], Xiangang Wang[1], Yves De Deene[2]
[1]Institute of Nuclear and New Energy Technology, Tsinghua University, Beijing, 100084, China
[2]The Biomedical Engineering Laboratory, Department of Engineering, Macquarie University, Sydney, 2109, Australia
[3]Department of Radiation Oncology, Fudan University Shanghai Cancer Center, Shanghai, 200032, China

E-mail: wangxiangang@tsinghua.edu.cn

Abstract. Two types of angular rotation deviations are observed in our optical CT scanner for gel dosimetry: a large deviation at the starting position, and small deviations during the scanning. In order to investigate the influence of these angular rotation deviations on the reconstructed OD maps, we applied the angular deviations on a synthetic phantom for optical CT simulation. Meanwhile, three reconstruction schemes are proposed for compensation. The simulation results show that the influence of both types of rotation deviation is as small as less than 1% over the central reconstruction phantom region. Based on the reconstructed results via different methods, we can conclude: 1) reconstruction with the regridded projections can better decrease the errors caused by the large angle deviation; 2) for small angle deviations, reconstruction with actual-angle compensation delivers less pronounced results; 3) for real cases, the hybrid approach is shown to reduce reconstruction errors.

1. Introduction

Gel dosimetry has received increasing research interest for its outstanding volumetric dose distribution measurement performance [1-4]. Optical CT, utilizing the quantitative optical density changes induced by absorbing dose, has been proposed as an alternative readout method to MRI [5-7]. An in-house dual-wavelength optical CT scanner for radiochromic gel dosimeter imaging has been developed [8]. In a typical optical CT scanning, the gel phantom is rotated slowly step by step with projections at different acquired. When projections over 360 degrees are acquired, tomographic images of the optical densities(ODs) of the gel phantom can be reconstructed by either filtered backprojection or iterative reconstruction algorithms. In each step of the optical CT imaging chain, errors may occur that lead to overall uncertainties on the reconstructed dose maps [9]. One of these errors involves the deviations of the angular increments by the stepper motor have been observed.

In this study, we discuss the influence of these angular deviations on the accuracy of the OD maps.
in projection angles induced by the optical CT phantom rotation system.

2. Methods and Materials

2.1. Rotation Deviation Analysis

The rotation control program is in-house developed in *Matlab*. For typical optical CT scanning, projections are obtained over 360 degrees with an angular increment of 1 degree. However, in practice small deviations from its target rotation angles are observed. We measured the deviations in rotation angles over 20 scans, and Figure 1(a) shows the rotation angle deviation curves in three typical scans. We can see that in most cases the actual projection angles are equal to the respective aimed ones within 0.1 degree deviations. Only a small portion of actual angles deviate more than 0.1 degree, and all deviations are negative, i.e. the actual rotation angle lags behind the rotation angle target.

Based on different locations and amplitudes, we can classify the deviations into two categories: a) at the starting zero angle, the deviation is relatively as large as around -1.9 degree as in Figure 2(a); b) during scanning, rotation deviations always appear as -0.1 degree at random angles. For the former type a) deviation, since it always takes place at the initial state, we assume that there is kind of intrinsic starting or initialization error in the stepper motor. For the latter type b) deviation, the amplitude is constant, but the frequency and position of occurrence are random as in Figure 2(b).

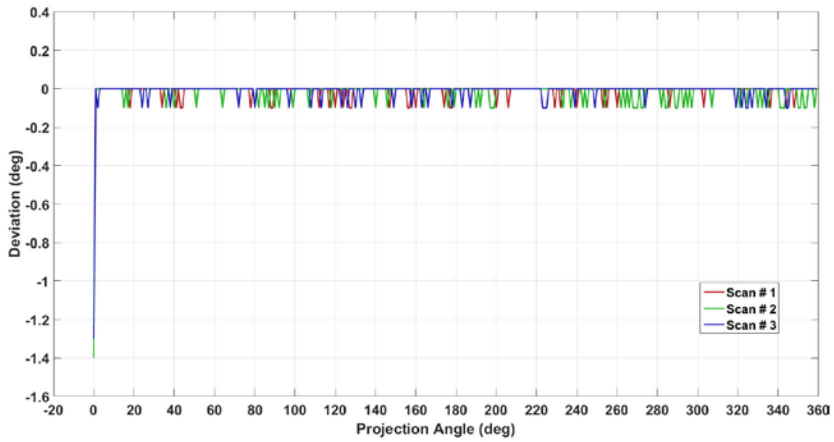

Figure 1. The rotation deviations from aimed angles in three typical experiment scans.

2.2. Deviation Modelling for Simulation

In order to assess the influence of rotation deviations to the OD maps, we used a synthetic circular phantom with square field [10]. For optical CT imaging simulation, all the geometric parameters were identical to the dual-wavelength optical CT scanner specifications [11]. In the rotation deviation simulation part, we first generated 360 exact projection angles from 0 to 359 with 1-degree interval. Then a series of numbers were generated via a deviation model, and added to the exact angle series to mimic rotation deviated angles.

We launched two simulation scenarios to assess the influence of the two types of deviations respectively, and in both scenarios we pushed the boundaries of the deviations to make them much worse than the real case. For the type a) deviation, it only happens at the initial state with a large amplitude as in Figure 2(a). The mean deviation over 20 scans is -1.5 degree, and the worst case -1.9 degree. Herein, we set the amplitude to -3 degree constantly and 6 deviations in random positions. For the type b) deviation, it occurs randomly during rotation as in Figure 2(b) but the amplitude is constant to -0.1 degree. The mean deviation count is 38.95, and the standard deviation is 11.96. To push it to the limit, we introduced a constant -0.1 degree deviation at 180 random projection angles.

2.3 Reconstruction Strategies

The classical cone-beam filtered backprojection algorithm (FDK) with a Hann filter is used for its advantageous performance in noise suppression and gradient integrity [10].

To compensate for the angular deviations, we proposed three schemes for reconstruction: 1) we reconstructed the deviated projections blindly as if there were no deviations at all; 2) for compensation, we used the actual rotation angles for backprojection in our FDK algorithm; 3) we regridded the missing projections by linear interpolation at the exact angles. As reference, exact projections with no rotation deviations were also reconstructed with FDK.

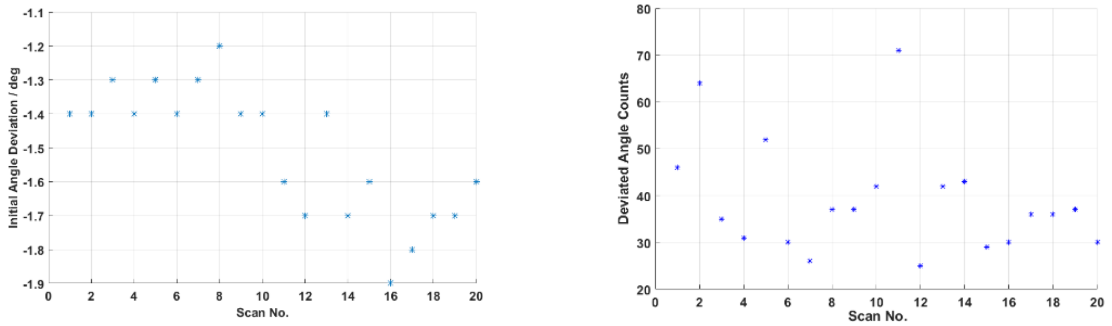

(a) (b)

Figure 2. (a) Initial angle deviations over 20 scans. (b) Counts of deviation angles over 20 scans.

3. Results and Discussion

3.1. Influence of Type a) Deviations

In this simulation, 6 angles deviated by -3 degree were generated by our Monte Carlo method, as shown in Figure 3(a). As described above, we used three reconstruction schemes: blind reconstruction, compensated reconstruction, regridded reconstruction. The comparative reconstructed results are shown in Figure 4. Note that the OD of the synthetic phantom matrix is 0.1, and the mean value OD of the central part of the square field is 0.26. The mean value of ΔOD in the central square field is about 0.16.

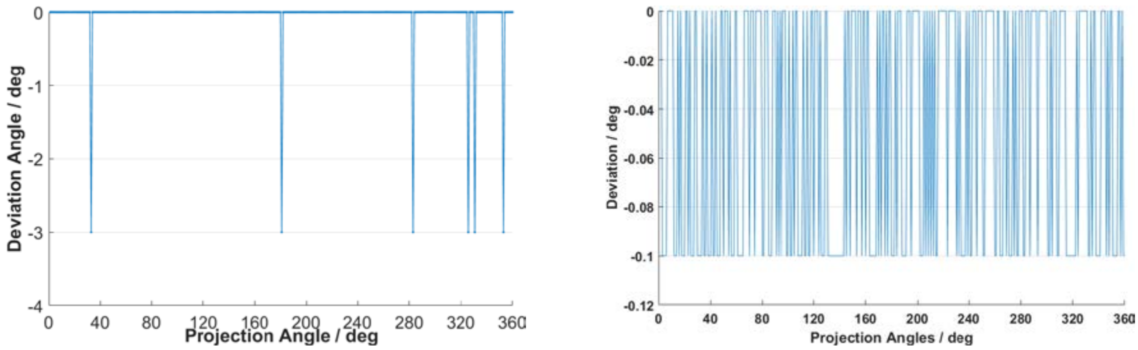

(a) (b)

Figure 3. The simulated type a) rotation deviation curve, and type b) rotation deviation curve.

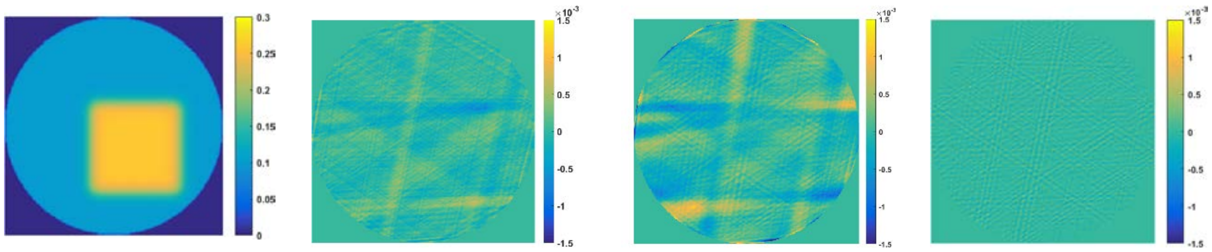

(a) (b) (c) (d)

Figure 4. (a) Reference FDK result of the middle slice with exact projections. (b) Difference map of the results between blind reconstruction and reference reconstruction. (c) Difference map of the results between

compensated reconstruction and reference reconstruction. (d) Difference map of the results between regridded reconstruction and reference reconstruction.

3.2. Influence of Type b) Deviations

In this simulation, 180 angles deviated by -0.1 degree were generated (shown in Figure 3(b)). The comparative reconstructed results of the middle tomographic slice by scheme methods are demonstrated in Figure 5. The deviation induced error will corrupt the dose gradient in larger extent, but effect is small with the largest error around 0.5%.

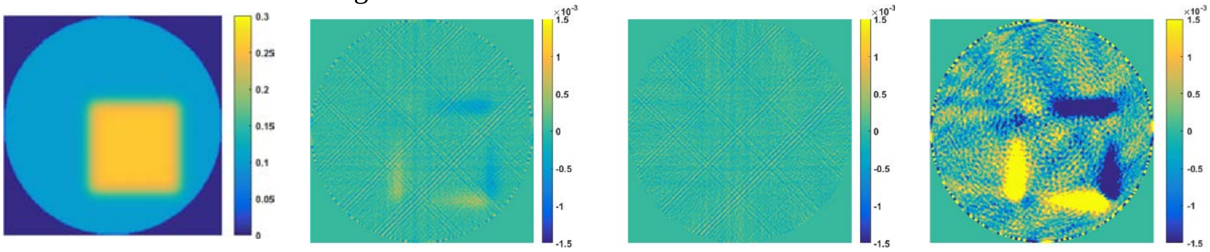

(a) (b) (c) (d)

Figure 5. (a) Reference FDK result of the middle slice with exact projections. (b) Difference map of the results between blind reconstruction and reference reconstruction. (c) Difference map of the results between compensated reconstruction and reference reconstruction. (d) Difference map of the results between regridded reconstruction and reference reconstruction.

3.3. Simulation Using Actual Angle Positions

From the comparison above, we can conclude that regriding reconstruction approach is effective for large angle deviation correction, and compensated reconstruction approach delivers better less affected results from small angle deviations. Herein, in order to assess the influence of angle deviations in a real case, we launched another simulation using actual angle positions from an experimental scanning record file, and adopted a hybrid reconstruction scheme: we first regridded the projection at the starting angle, and used compensated approach for reconstruction. As we conceive, this hybrid method gave the least influence results than the other methods, and the largest deviation in the reconstruction field is no more than 0.3% normalized by the mean value of ΔOD.

4. Conclusions

The results show that the influence of both types of rotation deviation is relatively small, less than 1% (normalized by the mean OD value of the square field) in most reconstruction area. The comparative results of different reconstruction schemes show: 1) reconstruction with regridded projections can better restore the ghost pattern caused by large angle deviation; 2) for small angle deviations, reconstruction with actual angle compensation gives less influenced results; 3) for real cases, a hybrid approach delivers results with least errors. The rationale of correction strategy suitability needs further comprehensive work. This study is based on our in-house scanner, and in the future we will use the proposed method to investigate the influence of rotation deviations in a generalized scenario. Also, we will use a hybrid iterative reconstruction algorithm, i.e. SART+OS+TV [12], which is upgraded from [13] to investigate its performance to rotation deviations.

5. Acknowledgement

Jointly Supported by the National Science Foundation of China (No. 61571262, No.11575095, No. 61171115), and the National Key Research and Development Program (No. 2016YFC0105406).

6. References

[1] Baldock C *et al* 2010 *Phys. Med. Biol.* **55** R1-63
[2] De Deene Y *et al* 2002 *Phys. Med. Biol*. **47** 2459
[3] De Deene Y and Baldock C 2002 *Phys. Med. Biol*. **47** 3117-41
[4] De Deene Y *et al* 2002 *Phys. Med. Biol*. **47** 3441-63

[5] Vandecasteele J and De Deene Y 2013 *Phys. Med. Biol.* **58** 19-42
[6] Vandecasteele J and De Deene Y 2013 *Phys. Med. Biol.* **58** 43-61
[7] Vandecasteele J and De Deene Y 2013 *Phys. Med. Biol.* **58** 63-85
[8] De Deene Y *et al* 2015 *Phys. Med. Biol.* **60** 1543-63
[9] De Deene Y and Jirasek A 2015 *J. Phys.: Conf. Ser.* **573** 012008
[10] De Deene Y 2015 *J. Phys.: Conf. Ser.* **573** 012076
[11] De Deene Y 2015 *J. Phys.: Conf. Ser.* **573** 012058
[12] Du Y *et al* 2016 *Phys. Med. Biol.* **61** 8425-8439
[13] Yi D *et al* 2015 *J. Phys.: Conf. Ser.* **573** 012063